Thevenin's Equivalent of Photovoltaic Source Models for MPPT and Power Grid Studies

A. Chatterjee, *Student Member, IEEE*, and A. Keyhani, *Fellow, IEEE*

***Abstract*–The model of a photovoltaic (PV) source is needed for Maximum Power Point Tracking (MPPT) and power grid studies. The single diode model can fairly emulate PV's characteristic. The only nonlinear element in this model is the single diode. This paper proposes Thevenin's equivalent model for a PV source by piecewise linearization of the diode characteristic. The variation of the parameters with the change in temperature and irradiance is also studied. It is shown that Thevenin's equivalent model of PV produces a voltage-current characteristic which represents the PV source operation fairly well.**

Index Terms: **Modeling, photovoltaics (PVs), power grid.**

I. Introduction

With the supply of fossil fuel dwindling and the threat of global warming looming large, alternative sources of energy have to be put into wider use. The European Union has set an objective of reaching a penetration of renewable energy of 12% [1]. Solar energy is a renewable source of energy which is available in abundance and can be converted into electrical energy directly by photovoltaic (PV) sources. The European Union is campaigning for one million PV systems with a total capacity of 1 GW (peak) by 2010 [1]. The increased penetration of the PV system necessitates a mathematical model, which can be used for the study of power grids [2].

A PV source has a non-linear voltage-current (V-I) characteristic, which can be modeled using current sources, diode(s), and resistors. Single-diode and double-diode models are widely used to simulate PV characteristics. The single-diode model emulates the PV characteristics fairly accurately. The manufacturer provides information about the electrical characteristics of PV by specifying certain points in its V-I characteristics, which are called remarkable points [3].

This paper uses the single-diode model to develop a Thevenin's equivalent model of PV. It first discusses the parameter estimation of a single-diode model for a given temperature and irradiance and then it discusses developing Thevenin's equivalent model by using those parameters.

As shown in Figure 1, the single diode model for PV consists of a current source representing the photo-generated current, a diode, and two resistances (series and parallel). From Kirchhoff's current law, the output current can be written as in (1) [4-6].

$$I = I_{ph} - I_0\left\{\exp\left(\frac{V + IR_s}{n_s V_t}\right) - 1\right\} - \frac{V + IR_s}{R_{sh}} \tag{1}$$

where V and I are the module output voltage and current, respectively; I_{ph} and I_o are the photo-generated current and the dark saturation current, respectively; V_t is the junction thermal voltage, R_s and R_{sh} are the series and parallel resistances, respectively; n_s is the number of cells in the module connected in series.

The thermal voltage of the diode is related to the junction temperature as given by (2),

$$V_t = \frac{kTA}{q} \tag{2}$$

where k is the Boltzmann's constant, T is the junction temperature, A is the diode quality factor, and q is the electronic charge.

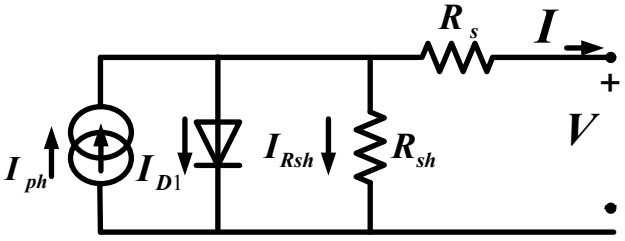

Fig. 1. The single-diode model of a PV source.

There are five unknown parameters in the single-diode model which need to be estimated before developing Thevenin's equivalent of the model. These unknown parameters are I_{ph}, I_o, V_t, R_s, and R_{sh}. The estimation of

978-1-4577-1002-5/11/$26.00 ©2011 IEEE

these parameters is performed from the information provided by the manufacturers' datasheet. Once the parameters are known, they are adjusted for the changing environmental conditions. With the parameters known, the model is linearized to obtain Thevenin's equivalent model of PV as seen back into PV from its output terminals. Other related papers are given in [7-11].

II. Parameter Estimation

The manufacturers' datasheet provides the remarkable points and the temperature coefficients of the voltage, k_v, and current, k_i. The remarkable points are points of interest on the V-I curve of PV at standard test condition (STC) which is usually a junction temperature of 25° C and an irradiance of 1000 Wm^{-2} [12]. The open-circuit voltage, V_{oc}, the short-circuit current, I_{sc} and the voltage, V_{mpp}, and current, I_{mpp}, at maximum power point (MPP) are provided from the datasheet. Using the above information, the five unknown parameters are estimated [3].

The estimation process is simplified by neglecting the '-1' in (1), since the exponential term is large compared to 1. Three equations, (3) through (5), are obtained from the V-I characteristic by substituting the remarkable points into (1). Since there are five unknown parameters, two more equations are needed.

$$I_{sc} = I_{ph} - I_o.\exp\left\{\frac{I_{sc}.R_s}{n_s.V_t}\right\} - \frac{I_{sc}.R_s}{R_{sh}} \tag{3}$$

$$I_{mpp} = I_{ph} - I_o.\exp\left\{\frac{V_{mpp} + I_{mpp}.R_s}{n_s.V_t}\right\} - \frac{V_{mpp} + I_{mpp}.R_s}{R_{sh}} \tag{4}$$

$$I_{oc} = 0 = I_{ph} - I_o.\exp\left\{\frac{V_{oc}}{n_s.V_t}\right\} - \frac{V_{oc}}{R_{sh}} \tag{5}$$

The next equation is derived from the power at the maximum power point, and therefore, the derivative of power with respect to voltage at that point is zero:

$$\left.\frac{dP}{dV}\right|_{\substack{V=V_{mpp}\\I=I_{mpp}}} = 0 \tag{6}$$

With four of the five equations formed, the fifth equation is formed from the slope of the V-I curve at short circuit point as shown in (7).

$$\left.\frac{dI}{dV}\right|_{\substack{V=0\\I=I_{sc}}} = -\frac{1}{R_{sho}} \tag{7}$$

It is observed that the value of R_{sho} is approximately equal to the parallel resistance, R_{sh} and the equation (7) is now written as in (8). Utilizing this fact, all of the five parameters can now be estimated from the information provided by the datasheet only.

$$\left.\frac{dI}{dV}\right|_{\substack{V=0\\I=I_{sc}}} \approx -\frac{1}{R_{sh}} \tag{8}$$

The variables above are now changed for systematic mathematical representation as listed in Table I.

TABLE I
List of Variable Transformations

Datasheet values		
I_{sc}	a_1	Short-circuit current
V_{oc}	a_2	Open circuit voltage
V_{mpp}	a_8	Voltage at MPP
I_{mpp}	a_4	Current at MPP
n_s	a_5	Number of cells in series in a module
Unknown parameters		
I_{ph}	x_1	Photo-generated current
I_o	x_2	Dark saturation current
V_t	x_3	Junction voltage
R_s	x_4	Series resistance
R_{sh}	x_5	Parallel resistance
R_{sho}	x_6	Effective resistance at short circuit
Output quantities of the PV source		
I	y_1	Output current
V	y_2	Output voltage
P	y_3	Output power

Simplifying the five equations, (3) through (6), and (8), in a method shown in [13], we arrive at five equations, (9) through (13), which are solved to obtain the parameters:

$$x_1 = x_2 \exp\left\{\frac{a_2}{a_5.x_3}\right\} + \frac{a_2}{x_5} \tag{9}$$

$$x_2 = \left(a_1 - \frac{a_2 - a_1 x_4}{x_5}\right)\exp\left\{-\frac{a_2}{a_5.x_3}\right\} \tag{10}$$

$$x_3 = \frac{a_4.x_4 + a_3 - a_2}{J} \tag{11}$$

where $J = a_5.\log\left(\frac{a_1x_4 + a_1x_5 - a_4x_4 - a_4x_5 - a_3}{a_1x_4 + a_1x_5 - a_2}\right)$

$$x_4 = \frac{a_2 - a_3 + a_5x_3.\ln(M)}{a_4} \tag{12}$$

where

$$M = \frac{a_5x_3.(a_4x_4 + a_4x_5 - a_3)}{a_1x_4a_3 + a_1x_5a_3 + a_4a_2x_4 - a_4a_1x_4^2 - a_4a_1x_5x_4 - a_3a_2}$$

$$x_5 = \frac{a_5x_3x_4 + a_5x_3x_5 + N}{a_5x_3 + N} \tag{13}$$

where $N = x_4.\exp\left\{\frac{a_1x_4 - a_2}{a_5x_3}\right\}.(a_1x_4 + a_1x_5 - a_2)$.

It is seen that equations (11) through (13) are transcendental equations, whereas (9) and (10) are not. Therefore, the solution of the above equations reduces down to a numerical solution of three equations and then we use the parameters found to obtain the values of the remaining two parameters of (10) and (9), respectively.

III. Case Study

A case study to find the parameters of the PV module produced by Mitsubishi Electric, PV-MF165EB3, was conducted at STC and at varying environmental conditions. Table II lists the values provided on the datasheet, followed by the values of the estimated unknown parameters.

TABLE II
DATASHEET VALUES AND ESTIMATED PARAMETERS OF A MODULE

Datasheet Values		Estimated Parameters	
I_{sc}	*7.36 A*	I_{ph}	*7.36 A*
V_{oc}	*30.4 V*	I_o	*0.104 μA*
V_{mpp}	*24.2 V*	A	*1.310*
I_{mpp}	*6.83 A*	R_s	*0.251 ohm*
n_s	*50*	R_{sh}	*1168 ohm*
Temperature coefficients			
K_i	*0.057%*	K_v	*-0.346%*

IV. Temperature and Irradiance Dependence

The V-I characteristics of PV change with the change in the irradiance and the junction temperature. The development of power in PV, as a result of irradiance on it, is modeled in the single diode model as the current source represented by the photo-generated current. As a result, the photo-generated current is directly proportional to the irradiance as given in (14). And since the short circuit current is directly proportional to the photo-generated current, equation (15) follows:

$$x_1(G) = x_1(G_{stc}).\frac{G}{G_{stc}} \tag{14}$$

$$a_1(G) = a_1(G_{stc}).\frac{G}{G_{stc}} \tag{15}$$

where G is the irradiance on the module and G_{stc} is the irradiance on the module at STC.

The open-circuit voltage, however, is not directly proportional to the irradiance: rearranging (9), the open-circuit voltage, as a function of irradiance is given by (16).

$$a_2(G) = a_5.x_3\ln\left(\frac{x_1(G).x_5 - a_2(G)}{x_2.x_5}\right) \tag{16}$$

The manufacturer's datasheet provides the temperature coefficients of both short-circuit current and open-circuit voltage as in (17) and (18), respectively [13].

$$x_1(T) = x_1(T_{stc}) + K_i(T_{stc} - T) \tag{17}$$

$$x_2(T) = x_2(T_{stc}) + K_v(T_{stc} - T) \tag{18}$$

The dark saturation current of the diode is a function of temperature only. Its value at a given temperature is derived by expressing the terms in (10) as a function of temperature, as given in (19).

$$x_2(T) = \left(a_1(T) - \frac{a_2(T) - a_1(T)x_4}{x_5}\right)\exp\left\{-\frac{a_2(T)}{a_5.x_3}\right\} \tag{19}$$

The photo-generated current is also a function of temperature, and its value at a given temperature is found by writing the terms in (9) as functions of temperature as given in (20).

$$x_1(T) = x_2(T)\exp\left\{\frac{a_2(T)}{a_5.x_3}\right\} + \frac{a_2(T)}{x_5} \tag{20}$$

Following (14) through (20), the parameters of the PV which change with temperature and irradiance are adjusted. It should be noted that the photo-generated current and the dark saturation current are the only two parameters which change with temperature and irradiance. The other parameters remain unaffected.

V. Linearization of Diode

The only non-linear element in the model shown in Figure 1 is the diode. The voltage and current (V-I) in a diode are related by an exponential relationship as given by Shockley and is given in (21) [14]:

$$I_D = I_o\left\{\exp\left(\frac{v_D}{n_s.V_t}\right)-1\right\} \tag{21}$$

where V_D and I_D are the diode voltage and current, respectively.

The piecewise linearization is used to linearize the diode as shown in Figure 2. In this technique, the function is divided into a number of small regions. In each region, a straight line is used to closely approximate the actual nonlinear function, as shown in Figure 2. It is assumed that the non-linear function can be approximated by the straight line in that region.

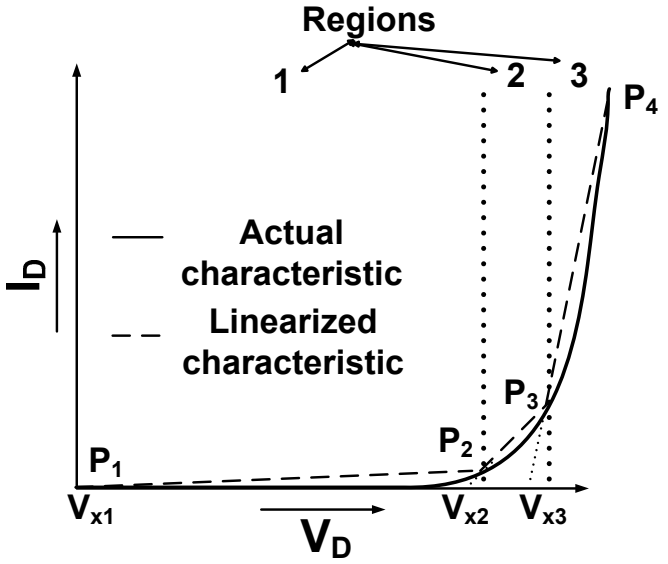

Fig. 2. Voltage current characteristic of diode showing actual characteristic and the linear approximation [14].

In Figure 2, the diode characteristic has been approximated by dividing its characteristic into three regions, in each of which a diode is represented by a straight line. In terms of circuit, each of these lines can be approximated by a voltage source V_x and a resistance R_D. The voltage source V_x is actually the voltage axis intercept of the straight lines represented by V_{x1}, V_{x2}, and V_{x3} in Figure 2 for regions 1, 2, and 3 respectively. The resistance R_{D1}, R_{D2}, and R_{D3} are the inverse of the slope of the lines in each region. It goes without saying that as the number of regions is increased, the piecewise linearization approximates the actual diode characteristic more closely, decreasing the error caused by the approximation.

The PV model, where the diode is linearized, is shown in Figure 3. The value of R_D and V_x will depend on the region of operation.

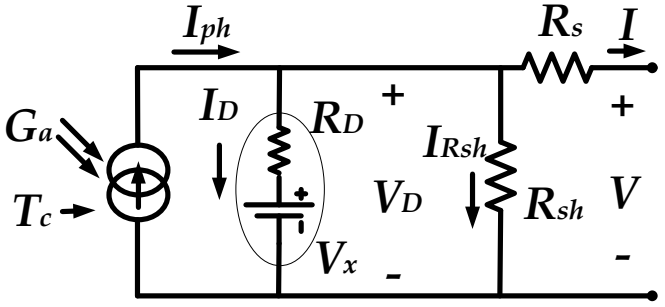

Fig. 3. PV model with diode linearized

The linearized model of Figure 3 can now be represented by Thevenin's equivalent voltage and resistance given by (22) and (23):

$$V_{Th,i} = V_{x,i} + R_{D,i}.\frac{I_{ph}.R_{sh} - V_{x,i}}{R_{sh} + R_{D,i}} \tag{22}$$

$$R_{Th,i} = R_s + \frac{R_{sh}.R_{D,i}}{R_{sh} + R_{D,i}} \tag{23}$$

where, $V_{Th,i}$ and $R_{Th,i}$ are Thevenin's equivalent voltage and resistance of the model of Figure 3 at region i (i = *1, 2, ...number of regions*). Thevenin's equivalent circuit of the PV looking back from its output terminals is shown in Figure 4.

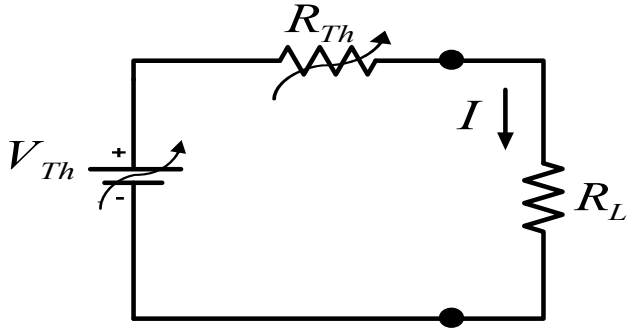

Fig. 4. Thevenin's equivalent circuit of PV

The piecewise linearization is an approximation technique, which has inherent error at points which do not coincide with the actual function. It is only those points given by the boundaries of the regions where the approximation exactly matches with the original function. Hence, at the boundaries of the regions, the error is zero.

The PV source is controlled to operate at maximum power point. Hence, it is desired that the approximation is error free at the point of operation. Therefore, one of the boundaries is chosen at MPP. Other boundaries can be either distributed evenly over the voltage range of operation or chosen, such that the error is minimal.

VI. Voltage-Current Characteristic of PV

Once the five parameters of the PV are determined, the diode characteristic defined by A and I_o is also known. From the maximum power point of PV, the corresponding point on the diode voltage-current characteristic is also determined. One of the points for linearization is chosen at this point on the diode characteristic, so that when maximum power point tracking (MPPT) is applied, PV operates on the exact MPP instead of the approximated point. The other points are chosen on either side of the PV characteristics. More points are chosen on the right side of the PV characteristics as it is more curved and lesser on the left, as the characteristic is almost linear.

Since the relationship between the output voltage and current of PV is implicit, a numerical solution is needed to obtain the value of current at a given voltage. Several computational and simulation methods of voltage current characteristics are found in the literature [15-18]. But with the linearization of the diode characteristic and obtaining Thevenin's equivalent circuit of PV, the numerical solution is avoided.

VII. Simulation Results

Thevenin's equivalent model of PV is simulated at various temperatures and irradiances to see the effect of linearizing the diode characteristic of PV. The error in the approximation is plotted to show its accuracy. Here, the linearization has been done with ten points of linearization between zero and open circuit voltage. This means that there are nine regions with different Thevenin's voltages and resistances.

Figure 5 shows the voltage-current and voltage-power characteristic of PV for both the actual case and Thevenin's equivalent at STC along with the percent error in the plot for Thevenin's equivalent model. Table III lists the Thevenin's equivalent voltage and resistance at STC and for different values of currents.

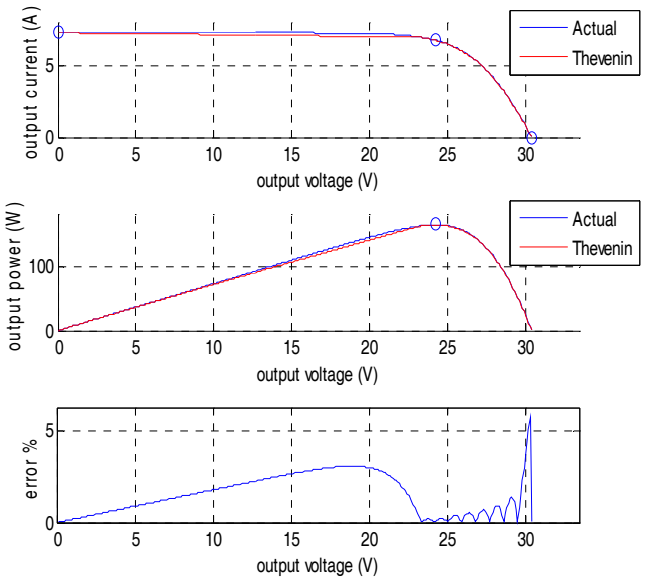

Fig. 5. Plot of Thevenin's equivalent circuit in comparison with the actual response at STC (25° C and 1000 Wm^{-2})

TABLE III

Thevenin's Voltage and Resistance for 25° C and 1000 $W m^{-2}$

T = 25° C, G = 1000 Wm^{-2}		
Output current, A	Thevenin's voltage, V	Thevenin's resistance, Ω
0 to 0.9624	*42.1000*	*1.2469*
0.9624 to 1.7514	*42.3638*	*1.5210*
1.7514 to 2.3709	*43.0926*	*1.9371*
2.3709 to 2.8361	*44.6160*	*2.5797*
2.8361 to 3.1709	*47.4633*	*3.5836*
3.1709 to 3.4033	*52.4730*	*5.1635*
3.4033 to 3.5600	*60.9636*	*7.6583*
3.5600 to 3.6634	*74.9968*	*11.6002*
3.6634 to 3.8700	*608.9235*	*157.3446*

Figure 6 shows the voltage-current and voltage-power characteristic of PV for both the actual case and Thevenin's equivalent at 25° C and 200 Wm^{-2} along with the percent error in the plot for Thevenin's equivalent model. Table IV lists the Thevenin's equivalent voltage and resistance at the above conditions and for different values of currents.

Figure 7 shows the voltage-current and voltage-power characteristic of PV for both the actual case and Thevenin's equivalent at 100° C and 1000 Wm^{-2}, along with the percent error in the plot for Thevenin's equivalent model. Table V lists the Thevenin's equivalent voltage and resistance at the mentioned conditions and for different values of currents.

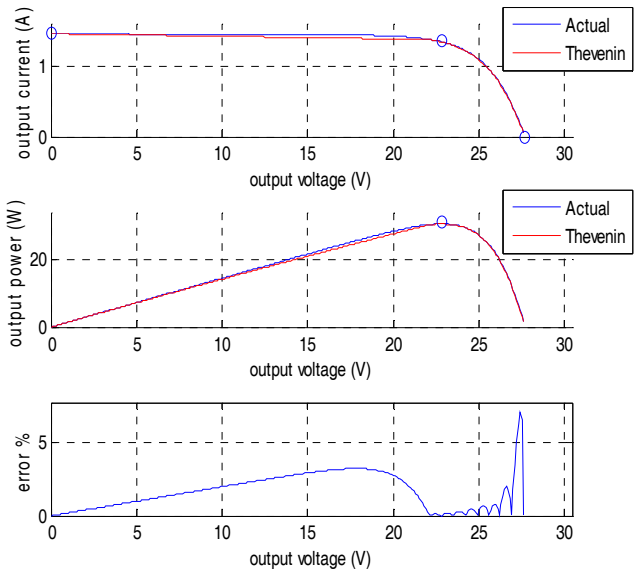

Fig. 6. Plot of Thevenin's equivalent circuit in comparison with the actual response at 25° C and 200 Wm^{-2}

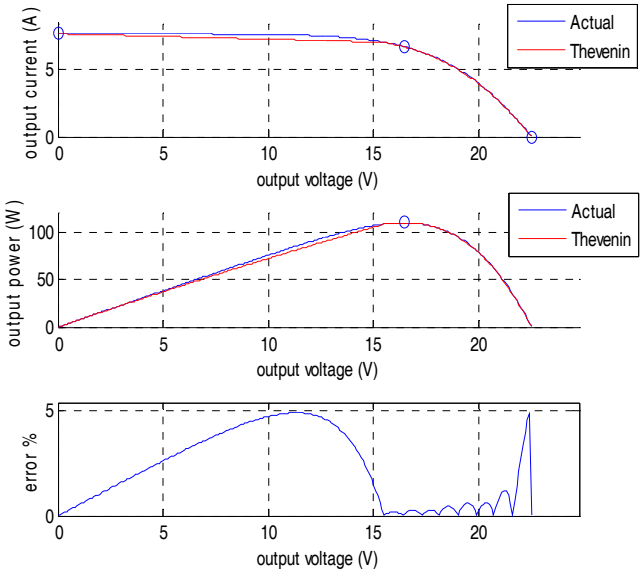

Fig. 7. Plot of Thevenin's equivalent circuit in comparison with the actual response at 100° C and 1000 Wm^{-2}

TABLE IV

THEVENIN'S VOLTAGE AND RESISTANCE FOR 25° C AND 200 $W m^{-2}$

T = 25° C, G = 200 Wm^{-2}		
Output current, A	Thevenin's voltage, V	Thevenin's resistance, Ω
0 to 0.2320	*37.8812*	*4.6605*
0.2320 to 0.3879	*38.2880*	*6.4143*
0.3879 to 0.4896	*39.2314*	*8.8464*
0.4896 to 0.5708	*40.9328*	*12.3213*
0.5708 to 0.6275	*43.9640*	*17.6319*
0.6275 to 0.6669	*48.8218*	*25.3733*
0.6669 to 0.6942	*56.3153*	*36.6094*
0.6942 to 0.7132	*67.5644*	*52.8133*
0.7132 to 0.7740	*380.3989*	*491.4715*

TABLE V

THEVENIN'S VOLTAGE AND RESISTANCE FOR 100° C AND 1000 $W m^{-2}$

T = 100° C, G = 1000 Wm^{-2}		
Output current, A	Thevenin's voltage, V	Thevenin's resistance, Ω
0 to 0.9388	*36.1001*	*1.3849*
0.9388 to 0.7151	*36.3720*	*1.6745*
0.7151 to 2.2936	*37.0576*	*2.0743*
2.2936 to 2.7843	*38.3764*	*2.6493*
2.7843 to 3.1286	*40.7044*	*3.4854*
3.1286 to 3.4051	*44.5086*	*4.7013*
3.4051 to 3.5902	*50.5825*	*6.4851*
3.5902 to 3.7332	*59.9197*	*9.0851*
3.7332 to 4.0587	*324.3096*	*79.9064*

It is seen from the plots shown in Figures 5 through 7 that Thevenin's equivalent model closely approximates the response of the single-diode model. The error is zero at the points of linearization. Since MPP is one of the points of linearization, the error is also zero at that point. PV is controlled to operate at MPP; therefore, Thevenin's model leads to an operation at the exact MPP. The error between two points of linearization increases and reaches a maximum of 7% for 25° C and 200 Wm^{-2} at a point close to open circuit. This is a point where PV will seldom operate. The error near the MPP where PV is most likely to operate with MPP is negligible. Tables III through V tabulate Thevenin's equivalent voltage and impedance for different environmental conditions and as a function of output current.

The accuracy of the Thevenin's equivalent model is depends on the number of points chosen for linearization. The error in the Thevenin's equivalent model will decrease with an increase in the number points. There are several algorithms which can be employed to determine where exactly the points should be located. One of them locates the points based on the equal area of error. This means that the area under the error curve for all the regions should be the same. This ensures a good accuracy throughout the curve. However, this algorithm comes with higher degree of complication and requires iterative method of solving for the area of the error. Moreover, if this method is employed, the MPP may not be one of the points of linearization where the error is zero. Since the PV source is mostly operated at MPP, the error at that

point is desired to be zero. In the simulation shown here, the points are uniformly distributed on the voltage axis, between the MPP and the open circuit voltage. Most points are selected on the right side of the MPP because the curve is more nonlinear in this region. Only one point is selected between MPP and zero voltage. From Fig. 5 to 7, it is seen that the error is mostly small on the left hand side even when there is only one point to the left of the MPP. Whereas, the error is relatively high for the regions to the right of MPP. If the PV is not made to operate at the MPP, it is desired that it operates at a point to the right of it so that the voltage regulation of the PV is good. Therefore, more points for linearization should be placed on the right side to reduce the error in linearization.

VIII. Conclusion

Thevenin's equivalent model derived from the single-diode model closely approximates PV characteristics as seen from the simulation results. This paper proposes to piecewise linearize the diode characteristic to develop Thevenin's equivalent circuit of a PV source. The simulation results show that the error in Thevenin's equivalent model is negligible at the maximum power point, a point where PV is controlled to operate at a given irradiance and temperature. From the simulation, it is concluded that the developed Thevenin's equivalent model can be used for simulation to study the behavior of PV. The advantage of using this model is that it avoids a numeric solution of the V-I characteristics of PV.

References

[1] Energy for the Future: Renewable Sources of Energy—White Paper for a Community Strategy and Action Plan, Nov. 26, 1997.

[2] A. Keyhani, M. N. Marwali, and M. Dai, *Integration of Green and Renewable Energy in Electric Power Systems*, Hoboken, NJ: Wiley, 2010.

[3] M. G. Villalva, J. R. Gazoli, and E. R. Filho, "Comprehensive approach to modeling and Simulation of Photovoltaic Arrays," *IEEE Trans. Power Electronics*, vol. 24, no. 5, pp. 1198–1208, May 2009.

[4] H. S. Rauschenbach, *Solar Cell Array Design Handbook*. New York: Van Nostrand Reinhold, 1980.

[5] M. G. Villalva, J. R. Gazoli, and E. R. Filho, "Modeling and circuit based simulation of photovoltaic arrays," *Brazilian Journal of Power Electronics*, vol. 14, no. 1, pp. 35 – 45, Feb. 2009.

[6] Minwon Park, and In-Keun Yu "A novel real-time simulation technique of photovoltaic generation systems using RTDS," *IEEE Trans. Energy Conversion*, vol. 19, no. 1, pp. 164 – 169, Mar. 2004.

[7] O. Wasynczuk, "Modeling and Dynamic Performance of a Line-Commutated Photovoltaic Inverter System," *IEEE Review*, *Power Engineering*, vol. 9, no. 9 pp. 35 – 36, Sep. 1989.

[8] S. Rahman, and B. H. Chowdhury, "Simulation of photovoltaic power systems and their performance prediction," *IEEE Trans. Energy conversion*, vol. 3, no. 3, pp. 440 – 446, Sep. 1988.

[9] B. Galiana, C. Algora, I. Rey-Stolle, and I. G. Vara, "A 3-D model for concentrator solar cells based on distributed circuit units," *IEEE Trans. Electron Devices*, vol. 52, no. 12, pp. 2552 – 2558, Dec, 2005.

[10] Yun Tiam Tan, D. S. Kirschen, and N. Jenkins, "A model of PV generation suitable for stability analysis," *IEEE Trans. Energy Conversion*, vol. 19, no. 4, pp. 748 – 755, Dec. 2004.

[11] J. T. Bialasiewicz, "Renewable Energy Systems With Photovoltaic Power Generators: Operation and Modeling," *IEEE Trans. Industrial Electronics*, vol. 55, no. 7, pp. 2752 – 2758, Jul. 2008.

[12] W. Xiao, W. G. Dunford, and A. Capel, "A novel modeling method for photovoltaic cells," in *Proc. IEEE 35th Annu. Power Electron. Spec. Conf. (PESC),* 2004, vol. 3, pp. 1950 – 1956.

[13] D. Sera, R. Teodorescu, and P. Rodriguez, "PV panel model based on datasheet values," *IEEE International Symposium on Industrial Electronics*, pp. 2392 – 2396, Jun. 2007.

[14] Ray-Lee Lin, and Yi-Fan Chen "Equivalent Circuit Model of Light-Emitting-Diode for System Analyses of Lighting Drivers," *Industry Applications Society Annual Meeting 2009*, pp. 1 – 5

[15] M. Veerachary, "PSIM circuit-oriented simulator model for the nonlinear photovoltaic sources," *IEEE Trans. Aerosp. Electron. Syst.*, vol. 42, no. 2, pp. 735 – 740, Apr. 2006.

[16] M. C. Glass, "Improved solar array power point model with SPICE realization," in *Proc. 31st Intersoc. Energy Convers. Eng. Conf. (IECEC),* Aug. 1996, vol. 1, pp. 286 – 291.

[17] I. H. Atlas and A. M. Sharaf, "A photovoltaic array simulation model for matlab-simulink GUI environment," in *Proc. Int. Conf. Clean Elect. Power (ICCEP)*, 2007, pp. 341 – 345.

[18] R. C. Campbell, "A circuit based photovoltaic array model for power system studies," in *Proc. 39th North Amer. Power Symp. (NAPS),* 2007, pp. 97 – 101.

Abir Chatterjee (S'10) was born in Kolkata, India, in 1984. He received his B-tech. degree in Electrical Engineering from West Bengal University of Technology, India, in 2007 and his M-tech degree in Electrical Engineering from Indian Institute of Technology, Roorkee, India, in 2009.

He is currently pursuing his Ph.D. at The Ohio State University, Columbus, Ohio. His current research interest includes smart grid power systems, modeling and control of distributed energy generation, and green energy systems.

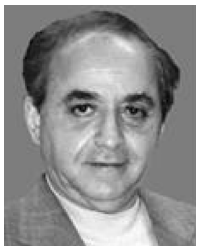

Ali Keyhani (S'72–M'76–SM'89–F'98) received the B.E., M.S.E.E., and Ph.D. degrees from Purdue University, West Lafayette, IN, in 1967, 1973, and 1976, respectively.

He is currently Professor of Electrical Engineering at The Ohio State University (OSU), Columbus, Ohio. He is also the Director of the OSU Electromechanical and Green Energy Systems Laboratory. From 1967 to 1972, he was with Hewlett-Packard Company and TRW Control, Palo Alto, CA. His current research interests include control of distributed energy systems, power electronics, multilevel converters, power systems control, alternative energy systems, fuel cells, photovoltaic cells, microturbines, distributed generation systems, and parameter estimation and control of electromechanical systems.

Professor Keyhani was the Past Chairman of the Electric Machinery Committee of IEEE Power Engineering Society and the Past Editor of the 3 University College of Engineering Research Award in 1989, 1999, and 2003.